



Universiteit
Leiden
The Netherlands

High fat diet induced disturbances of energy metabolism

Berg, S.A.A. van den

Citation

Berg, S. A. A. van den. (2010, October 6). *High fat diet induced disturbances of energy metabolism*. Retrieved from <https://hdl.handle.net/1887/16010>

Version: Corrected Publisher's Version

License: [Licence agreement concerning inclusion of doctoral thesis in the Institutional Repository of the University of Leiden](#)

Downloaded from: <https://hdl.handle.net/1887/16010>

Note: To cite this publication please use the final published version (if applicable).

Chapter 2: The hepatic lipid and plasma inflammatory marker profile of APOE3Leiden mice to high fat diets is characterized by a distinctly phased response.

Sjoerd A. A. van den Berg^{1,2,†}, Suzan Wopereis^{2,3,†}, Jorn R. de Haan^{2,3}, Uwe Thissen^{2,3}, Ivana Bobeldijk³, Louis M. Havekes^{2,3,4,5}, Ko Willems van Dijk^{1,2,4}, Ben van Ommen^{2,3}

1. Department of Human Genetics, Leiden University Medical Center, P.O. Box 9600, 2300 RC Leiden, The Netherlands
2. Nutrigenomics Consortium, Top Institute Food and Nutrition, P.O. Box 557, 6700 AN Wageningen, The Netherlands
3. TNO Quality of Life, P.O. Box 360, 3700 AJ Zeist, The Netherlands
4. Department of General Internal Medicine, Leiden University Medical Center, P.O. Box 9600, 2300 RC Leiden, The Netherlands
5. Department of Cardiology, Leiden University Medical Center, PO Box 9600, 2300 RC Leiden, The Netherlands

† Equally contributed to this publication

Manuscript submitted

Abstract

In rodent models, high fat diets are widely used to induce pathology associated with the metabolic syndrome. However, a variety of time frames and diets are used for the generation of specific pathology. Here, the etiology of high fat diet induced changes in plasma inflammatory markers as well as hepatic lipids was studied in ApoE3Leiden transgenic mice. High fat diets based on palm oil as well as beef tallow were used and the plasma inflammatory protein profile and hepatic lipid profile were determined on nine time points over a 16 week period. Multivariate statistical analyses revealed that the overall responses to both high fat diets were comparable and characterized by three distinct phases that were interpreted as an early acute phase response, an intermediate response and a late response characterized by hepatic lipid accumulation. However, after 16 weeks, the palm oil based high fat diet induced a significantly higher degree of whole body insulin resistance as compared to the beef tallow-based high fat diet. In addition, detailed analyses of the hepatic lipid profile revealed that, as compared to the beef tallow based high fat diet, the palm oil based high fat diet induced significantly increased hepatic levels of saturated versus mono-unsaturated lysophosphatidylcholines and increased levels of n-6 over n-3 poly-unsaturated free fatty acids. Our data demonstrate that the response of plasma inflammatory proteins and the hepatic lipid profile to high fat diets is not a linear continuum, but is characterized by distinct phases. Moreover, dietary fat source is a determinant of specific hepatic lipid composition and differentially affects whole body insulin sensitivity.

Introduction

The metabolic syndrome is defined by the co-occurrence of a series of risk factors for the development of type-2 diabetes and cardiovascular disease (282). These risk factors include obesity, increased blood pressure, increased fasting triglycerides, increased fasting glucose and decreased HDL-cholesterol. It is predicted that the current epidemic of obesity will lead to significant increases in the number of patients with the metabolic syndrome and thus to increased morbidity and mortality due to type-2 diabetes and cardiovascular disease.

Risk factors not included in the definition of the metabolic syndrome are hepatic lipid accumulation and low grade systemic inflammation, which are nevertheless both strongly associated with the metabolic syndrome (59;133). Hepatic lipid accumulation has been specifically associated with the presence of hepatic insulin resistance and dyslipidemia (136). Inflammatory processes in all metabolically active tissues have been associated with the pathology of the metabolic syndrome, including adipose tissue (178;261) and liver (128;136). Moreover, low grade inflammation, characterized by moderately increased levels of plasma inflammatory proteins, has been postulated to link metabolic syndrome with the vascular inflammatory phenotype of atherosclerosis (187). Despite these well described associations of systemic inflammation and hepatic lipid accumulation with the metabolic syndrome, there is relatively little insight in the etiology of systemic inflammation and hepatic lipid accumulation in the course of the development of the metabolic syndrome.

A commonly used model to study the pathology associated with the metabolic syndrome is the C57Bl/6 mouse fed a high fat diet containing 45-60 energy% fat. A variety of fat sources are being used in these studies (71;250;275) from both animal and plant origin. In addition, a variety of time frames are being applied, ranging from days to months. Thus, it is not always clear to what extent specific observations are affected by the selected diet and time frame. Moreover, wild type mice do not develop overt hyperlipidemia in response to high fat diets.

Here, we set out to gain insight in the timing of hepatic lipid accumulation and systemic inflammation in response to two different high fat diets by measuring the hepatic lipid profile and plasma markers of inflammation using a high frequency sampling approach. Two high fat (HF) diets composed of fat from plant and animal sources were used containing, respectively, 45 energy% Palm oil (HFP) and 45 energy% Beef Tallow (HFBT). As model, we selected the transgenic ApoE3Leiden (ApoE3L) mouse. ApoE3L mice are characterized by attenuated clearance of chylomicron and VLDL remnants. As a consequence, ApoE3L mice display a human-like lipoprotein metabolism, and are an established model for hyperlipidemia and atherosclerosis (as reviewed in (280)).

Our analyses showed that both high fat diets induced overall similar changes in plasma inflammatory markers and the hepatic lipid profile, that can be distinguished as three major subsequent phases: an early acute phase response (up to week 2), an intermediate response (week 4, 8) and a late lipid accumulation phase (week 12,16). Interestingly, the extent of insulin sensitivity after 16 weeks of high fat diet was significantly lower for the HFP diet as compared to the HFBT diet. This was associated with different levels of specific hepatic lipids containing mono-unsaturated fatty acids and the ratio between n3 and n6 polyunsaturated free fatty acids (PUFA) between the HFP and HFBT diets, which could play a role in the difference in the induction of impaired whole body insulin sensitivity observed between the two high fat diets.

Methods

Animals and diets

The study involved 186 male ApoE3L mice with an age of 14 ± 2 weeks at baseline. Animal experiments were approved by the Institutional Animal Care and Use Committee of the Netherlands Organization for Applied Scientific Research (TNO) and the Leiden University animal experimentation committee and were in compliance with European Community specifications regarding the use of laboratory animals.

The control group of ApoE3L mice was fed standard chow feed (RM3 (E) DU; Special Diet Services, Witham, Essex, UK), one group of ApoE3L mice was fed a high fat diet based on beef tallow (HFBT, 4032.05, Arie Blok B.V., Woerden, the Netherlands) and the third group of ApoE3L mice was fed a high fat diet based on palm oil (HFP). The HFP diet was based on an open source high fat lard diet (D12451, Research Diet Services, Wijk Bij Duurstede, the Netherlands), but the fat source was changed to palm oil. The macronutrients contents of these diets and the fatty acid composition are summarized in Table 1 and Table 2.

Study design

Before the start of the study, all the mice were fed a standard chow diet. At the start of the study, 62 mice were fed HFBT, 62 mice were fed HFP, and 62 mice stayed on the chow diet. In principle, 6 mice were sacrificed of each diet group at time points 1 and 3 days, 1, 2, 4, 8, 12, and 16 weeks. This study was part of a larger study in which also comprehensive liver transcriptomics analyses were performed (198).

Sample preparation

The animals were fasted for 4 hours before dissection. Typically, fasting started at 9:00 am and dissection at 1:00 pm. Animals were weighed and blood was collected by tail bleeding into chilled paraoxon (Sigma, St. Louis, USA)-coated capillary tubes to prevent in vitro lipolysis. Tubes were placed on ice and centrifuged, and the plasma was stored for total cholesterol, TG, and FFA

analysis. Subsequently, animals were sedated using isoflurane inhalation and plasma was collected from the retro-orbital plexus. This plasma was used for Rodent Map antigen analysis (Rules Based Medicine inc, Austin, TX, USA). Total cholesterol, TG, and FFA analysis was performed using commercially available enzymatic kits (Cat. No. 11489437216 and 11488872216; Roche Diagnostics, Almere, The Netherlands, and NEFA-C kit cat. No. 999-75406; Wako Chemicals GmbH, Neuss, Germany, respectively).

After exsanguination, animals were sacrificed by cervical dislocation and livers were harvested and snap frozen in liquid nitrogen as fast as possible. Tissues were kept at -180 °C before processing. For LC-MS of lipids and fatty acids, an accurate amount of lyophilized liver (approximately 5 mg) was extracted with 500 µl of isopropanol containing several internal standards (IS; C17:0_FFA; C17:0_LPC; C24:0_PC, C51:0_TG and C17:0-D-erythro-CER). For the lipid classes that are extracted and detected with this approach, see further description of the LC-MS methods. For LC-MS of lipids and fatty acids, a quality control (QC) sample was prepared by pooling aliquots of all individual liver extracts. The pool was divided over different aliquots. Additionally, from at least 10 samples two aliquots of liver were weighed and extracted separately. In this way, technical replicates were obtained.

Total liver lipid analysis

Extraction was performed using a modified Bligh and Dyer extraction protocol, optimized for steatotic liver material. In short, 50 mg of tissue was lysed in 100µl ice-cold methanol in a mini-bead beater (Biospec products) using glass beads. The homogenate was transferred to a new vial containing 450 µl of ice-cold methanol (J.T. Baker, cat. No. 8045) and homogenized again. Ice cold chloroform (J.T. Baker, cat. No. 7386) was added to obtain a 3:1 chloroform/methanol ratio and the mixture was homogenized. Homogenates were centrifuged at 4°C and 20.000 g for 15 minutes (Eppendorf 5417R). Supernatant was transferred and dried under a continuous nitrogen flow. A total of 100 µl of 2% Triton X-100 (Sigma Aldrich, cat. No. T8532) was added to the dried pellet to dissolve lipids. Samples were stored at 4°C until further processing. Triglyceride and cholesterol content was measured using enzymatic kits (Roche Diagnostics, cat. no. 11489437216 and 11488872216). Protein content was measured by bicinchoninic acid (BCA) analysis (BCA protein Assay Kit, Pierce, cat. No 23225). Liver lipid content was defined as total triglyceride content per mg of protein. In addition, total cholesterol level was measured in the same sample.

Hyperinsulinemic euglycemic clamp analysis

Whole body insulin sensitivity was measured by hyperinsulinemic euglycemic clamp analysis. Clamps were performed between 9:00 am and 11:00 am under overnight fasted conditions. Animals (Chow n=4, HFBT; n=8 and HFP; n=7) were under general anesthesia during the whole experiment, using a

Ventranquil/Dormicum/Fentanyl mixture. Glucose levels were determined by glucose hand meter measurements during the clamp. Insulin was infused at a rate of 3.5 mU/kg/min. Simultaneous infusion of glucose (12.5% glucose in PBS) was variable for each animal so that steady-state hyperinsulinemic plasma glucose levels were the same as baseline. Blood glucose levels were monitored every 10 minutes to ensure correct adjustments of the glucose infusion rate. Whole body insulin sensitivity was calculated by correcting the amount of glucose infused for body mass.

Plasma protein multiplex immunoassay measurements

Plasma collected from the retro-orbital plexus was used for analysis using the Plasma Antigens immunoassay panel included in the Rodent Multi-Analyte Profile as offered by Rules Based Medicine (Rules Based Medicine, Inc., Austin, Texas, USA) for measurement of expression levels of 71 proteins (RodentMAP version 2 antigen panel, see also table I, supplementary data).

For subsequent comparison analyses, biomarkers that showed no detectable expression (<LOW>) or expression beneath the least detectable dose (LDD) in more than half of the plasma samples were excluded from further data analysis ($\# <LOW> + \# <LDD> < 0.5 \times n$), unless at least 2 diet*time groups with 3 mice per group which are NOT (<LOW> or <LDL). In total 47 proteins were included in multivariate statistical analysis (see also table I, supplementary data). Included proteins that were reported with Quantity Not Sufficient (QNS) were replaced by '-1000', with <LOW> by $0.1 * LDD$, and with <LDL> by $0.5 * LDD$.

LC-MS of lipids and free fatty acids

Liver lipids and FFA were analyzed with electrospray LC-MS (19;62). The instrument used was a Thermo LTQ equipped with a Thermo Surveyor HPLC pump. Data were acquired by scanning the instrument from m/z 300 to 1200 at a scan rate of approximately 2 scans/s.

The lipid and FFA LC-MS platform employ the same HPLC conditions but different gradients. The lipids are separated on a Prosphere C4, 150 x 3.2 mm column with 5 μ m particles. Methanol water gradient with ammonium acetate and formic acid was used for elution. The detection of FFA is performed in negative ion mode whereas lipids are measured in positive ion mode. Together the two methods can detect approximately 200 different (abundant) identified lipids, FFA, TG, Lysophosphatidylcholine (LPC), Phosphatidylcholine (PC), Cholesterol ester (ChE) and Sphingomyelin (SPM). Phosphatidylserine (PS), Phosphatidylinositol (PI) and Phosphatidylethanolamine (PE) can not be detected with this approach. The FA chain composition of PC was determined by MS3. A selection of samples was re-injected and ionized in negative ionization mode. PC's form formiate adducts which are well detected and can be subjected to MS_n experiments, losing first the formiate and subsequently the FA anion which can be detected in

the spectra. The position of the double bonds can not be confirmed by this method but is proposed based on complementary biological information.

Each extract was injected three times, once for analysis with the LC-MS FFA platform and two times for analysis with the LC-MS lipid method, once without dilution and once after 50-fold dilution with isopropanol containing IS. The QC samples were distributed evenly between the study samples.

LC-MS of ceramides, sphingomyelins and diglycerides

Liver ceramides (CER), sphingomyelins (SPM) and diglycerides (DG) were analyzed with atmospheric pressure chemical ionization (APCI) LC-MS in the positive ion mode. The instrument used was a Thermo LT-FTMS equipped with a Thermo Surveyor HPLC pump. Data were acquired by scanning the instrument from m/z 300 to 1200 at a scan rate of approximately 1 scans/s. The detection was performed in the FTMS with resolution 10.000 at m/z 400. This platform employs the same HPLC conditions as the lipid method, described above. Each extract was injected once.

LC-MS spectral acquisition and data preprocessing

The LC-MS lipid profiling data were target-processed using the LC-Quan software (Thermo). A target table was prepared by searching chromatograms (all diet groups and all time points were represented) for all detectable lipid or FA peaks. For the lipids, a relative concentration (to the IS) was reported. In the ApoE3L liver samples, 59 different peaks could be identified with the LC-MS of lipids and free fatty acids method. In total 19 FFA (IS = C17:0_FFA), 6 LPC (IS used: C17:0_LPC, undiluted extract), 10 PC (IS used: C24:0_PC, undiluted extract), and 24 TG (IS used C51:0_TG, diluted extract). No SPM, monoglycerides, DG and CE were detected as concentrations were under the detection limit, even in the undiluted extract (see also table II, supplementary data). With the LC-MS of CER, SPM and DG method, 8 individual DG, 7 CER and 4 SPM (IS = C17:0-D-erythro-CER) were detected in the liver samples from this study (see also table II, supplementary data).

Outliers were identified and removed from the data. This was done by visual inspection of Principal Component Analysis (PCA) score plots for each platform. Mice that were clearly different from other measurements were marked as possible outliers. The data of these possible outliers were manually checked to confirm the measurement to be aberrant. Verified outliers were removed to prevent disturbing further data analysis.

In the original layout of the dataset, 6 mice were expected to be measured in every cell of the design matrix. However, due to a number of reasons data for 9 mice could not be obtained (5 measurement errors, 3 outliers, 1 peak integration problem).

To apply the ANOVA- Simultaneous Component Analysis (ASCA) algorithm (see section Statistical Analysis below), the design has to be balanced. Therefore equal numbers of mice needed to be present in the data cells. Consequently, missing measurements were estimated by randomly drawing samples from normal distributions, which were generated from the mean and standard deviation of the remaining measurements in the data cell. The samples were drawn for each metabolite and the resulting estimated measurements were then added to the data and included in the analysis.

Based on the relative standard deviations (RSDs) of the QC samples and technical replicates combined with a visual inspection, the data quality was considered to be good for both datasets.

Statistical analyses

To include the correlations that existed between the different lipids or proteins, the multivariate statistical technique ANOVA Simultaneous Component Analysis (ASCA) was applied (118;223). Similar to ANOVA, ASCA divides data into separate blocks of experimental factors on which a focused multivariate analysis is performed. This is done by simultaneous component analysis which -in this paper (and in most situations)- is equivalent to PCA (116). PCA represents the data by a reduced number of constructed variables (principal components or PCs), which gives the best explanation of the variation present in the data. This leads to an indication of the specific influence of a factor in the data (an effect) together with the lipids or proteins that are most important for this effect.

The scores of the first (or higher) PCs are then used to visualize the pattern present in a specific effect matrix. The loadings of the lipids and/or proteins in this PC can be described as a measure of the contribution of a lipid or protein to this PC. Lipids or proteins with the highest loadings were selected for further interpretation. As a preprocessing method, autoscaling was performed on the individual data blocks (diet, time and interaction) prior to PCA, to focus on relative changes rather than on metabolites with high variation which is often irrelevant (249). As a result, the amount of explained variance in lower PCs was substantial.

The significance (p-value) of the effects modeled by ASCA (diet effect, time effect or diet * time interaction effect) was estimated by permutation analysis of the data (257). The resulting distribution of sums of squares was compared with the observed one and a number of 1000 permutations were used for each effect.

Differences between the two high fat diets were assessed by performing ASCA on data normalized for chow (lipid & protein profiling data). In addition, to detect similar time effects in the lipid profile of ApoE3L mice on both high fat diets,

ASCA was performed on data normalized for chow. These ratios were generated by dividing every individual measurement by the median value of the control diet at the corresponding time point and taking the (2 base) logarithm. ASCA calculations were performed in Matlab 7.3.0.267 (The Mathworks Inc., Natick, MA, USA) with adapted Matlab scripts based on ASCA Matlab code, which was available online (Biosystems Data Analysis, Swammerdam Institute for Life Sciences, University of Amsterdam, www.bdagroup.nl).

Plasma TG, FFA, cholesterol, as well as body weight, liver lipid content and clamp data are represented as mean \pm SD. These data were analyzed using a parametric t-test by assuming equal variances. The thresholds for significance are set at a p-value of 0.05

Results

To determine the etiology of high fat diet induced changes in plasma inflammatory markers and hepatic lipid accumulation, three diets were used; a control chow diet, a high fat diet based on palm oil (HFP) and a high fat diet based on beef tallow (HFBT). The lipid compositions of the three diets used were analyzed by lipid profiling (table 1 and 2). The chow diet contained 7% lipids (13 energy%), and the two high fat diets contained 24% lipids (45 energy%). Both high fat diets were mainly rich in the fatty acids oleic acid (C18:1 ω 9) and palmitic acid (C16:0) and C50:1 and C52:2 TG compared to the chow diet. The HFP and HFBT diets differed mainly in the level of palmitoleic acid (C16:1; 14-fold higher in the HFBT diet), stearic acid (C18:0; 3-fold higher in the HFBT diet) and linoleic acid (C18:2 ω 6; 2-fold higher in HFP). The HFBT diet lacked the FA alpha linolenic acid (C18:3 ω 3). Furthermore, the HFBT diet contained 0.25% cholesterol.

Table 1: Macronutrient composition of control diet (chow) and high fat diets (HFBT and HFP).

Macronutrients (g/100 g)	Chow	HFBT	HFP
Protein	20.0	24.0	23.3
Carbohydrate	63.0	39.0	40.2
Fat	7.0	24.3	23.6
Fiber	5.0	6.0	5.8
Other	5.0	6.7	7.1
Total	100	100	100

Table 2: Fatty acid and triglyceride composition of the chow and high fat diets (HFBT and HFP).

Lipids (g/100 g fat)	Chow	HFBT	HFP
Fatty acids			
C12:0		-	0.3
C14:0		0.8	0.9
C16:0	10.0	28.9	35.4

C16:1w7		2.8	0.2
C18:0	3.8	14.8	4.4
C18:1w9	21.0	42.9	40.4
C18:2w6	52.0	8.8	16.4
C18:3w3	4.8	-	0.7
C20:0	0.5	-	0.5
C20:1w9	0.2	-	0.1
C22:0	0.5	-	0.2
cholesterol		1.0	-
Triglycerides			
C48:0_TG	0.5	2.3	1.0
C48:1_TG	0.4	4.5	1.2
C48:2_TG	0.4	1.2	0.3
C50:0_TG	0.4	3.9	4.8
C50:1_TG	1.7	16.5	27.8
C50:2_TG	3.6	6.5	8.1
C50:3_TG	0.8	1.0	0.4
C51:0_TG	0.5	1.5	0.4
C52:2_TG	3.7	27.9	23.0
C52:3_TG	9.6	5.8	10.1
C52:4_TG	13.6	1.0	3.1
C52:5_TG	2.6	0.1	0.3
C54:2_TG	0.9	15.7	1.9
C54:3_TG	5.1	7.9	6.3
C54:4_TG	8.3	1.7	4.0
C54:5_TG	16.6	0.3	3.1
C54:6_TG	17.3	0.2	2.2
C56:5_TG	5.1	0.1	0.4
C56:6_TG	6.3	0.1	0.5
Other	2.6	1.8	1.1

The effect of high fat diets on whole body physiology

At the start of the study, 186 male ApoE3L mice with an age of 14 ± 2 weeks were divided over three groups; 62 mice were fed HFP, 62 mice were fed HFBT, and 62 mice remained on the chow diet. From each diet group, 6 mice were sacrificed at time points 1 and 3 days, and at 1, 2, 4, 8, 12, and 16 weeks.

Body mass increased significantly on both high fat diets. As compared to mice on the chow diet, mice on the HFP diet were significantly more obese at time point 12 and 16 weeks, and mice on the HFBT diet were significantly more obese at time point 16 weeks. No significant differences in body weight were found between the two high fat diets at any time point (Figure 1).

Plasma analysis revealed that total plasma cholesterol level was increased in both high fat diet groups from the first day on, and remained significantly elevated for the duration of the experiment (Figure 2A). At time points 2 and 8 weeks, the HFP intervention group showed significantly higher cholesterol levels compared to HFBT. Plasma TG levels were elevated only at the first day of the experiment in both high fat diet groups (Chow; 1.2 ± 0.3 , HFP; 2.9 ± 1.5 and HFBT; 2.8 ± 1.2 mmol/l, Figure 2B). FFA levels showed a similar pattern, with only a transient increase during the first day (data not shown).

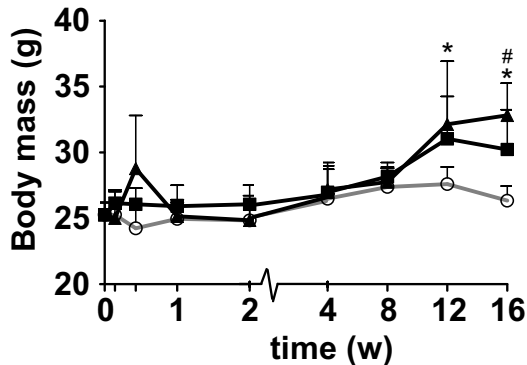


Figure 1: Average body mass of ApoE3L mice fed a chow (open circles, grey line), HFBT (squares) or HFP (triangles) diet. Lines represent means \pm SD. *: $p < 0.05$ for HFP compared to chow fed mice, #: $p < 0.05$ for HFBT compared to chow fed mice.

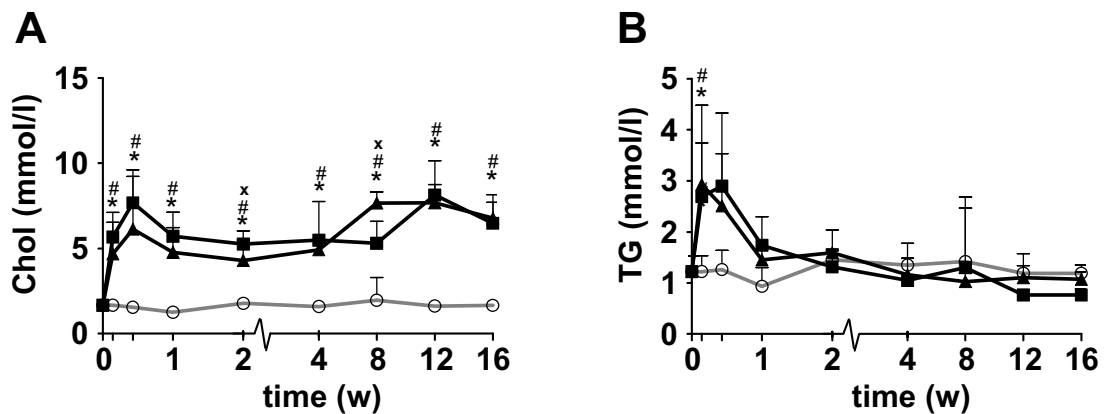


Figure 2: Average plasma cholesterol (Chol, A) and triglyceride (TG, B) levels of ApoE3L mice fed a chow (open circles, grey line), HFBT (squares) or HFP (triangles) diet. Lines represent means \pm SD. *: $p < 0.05$ for HFP compared to chow fed mice, #: $p < 0.05$ for HFBT compared to chow fed mice.

Whole body insulin sensitivity was determined by hyperinsulinemic euglycemic clamp analysis in a separate group of mice after 16 weeks of high fat diet intervention. Fasting plasma glucose levels were significantly elevated in both high fat groups compared to chow, and significantly higher in the HFP group compared to the HFBT group (Chow 7.5 ± 1.8 , HFBT; 10.6 ± 1.3 and HFP; 14.2

± 1.9 mmol/l, $p < 0.05$). Steady state hyperinsulinemic glucose infusion rates (GIR) at euglycemia were 2.4 times lower in HFBT group ($p = 0.03$) and 5.7 times lower in the HFP group ($p < 0.01$) compared to the chow fed group (Figure 3A and B). In addition, whole body insulin sensitivity was significantly more reduced in the HFP group compared to the HFBT group ($p < 0.01$) (GIR chow 117 ± 19 , HFBT; 51 ± 21 and HFP; 19 ± 15 $\mu\text{mol}/\text{kg} \cdot \text{min}$). Since HFBT and HFP fed animals were more obese than chow fed controls, which may influence the results, uncorrected glucose infusion rates (not corrected for body mass) are also reported. Uncorrected GIR remained significantly reduced in the HFBT and HFP group compared to chow fed controls, and were more reduced in the HFP fed group compared to the HFBT fed group (GIR chow 195 ± 16 , HFBT; 102 ± 39 and HFP; 38 ± 30 $\mu\text{mol}/\text{min}$, $p < 0.01$ chow versus HFBT, chow versus HFP and HFBT versus HFP, respectively). Thus, after 16 weeks of HF feeding, ApoE3L mice on both HF diets develop obesity, hypercholesterolemia and reduced insulin sensitivity.

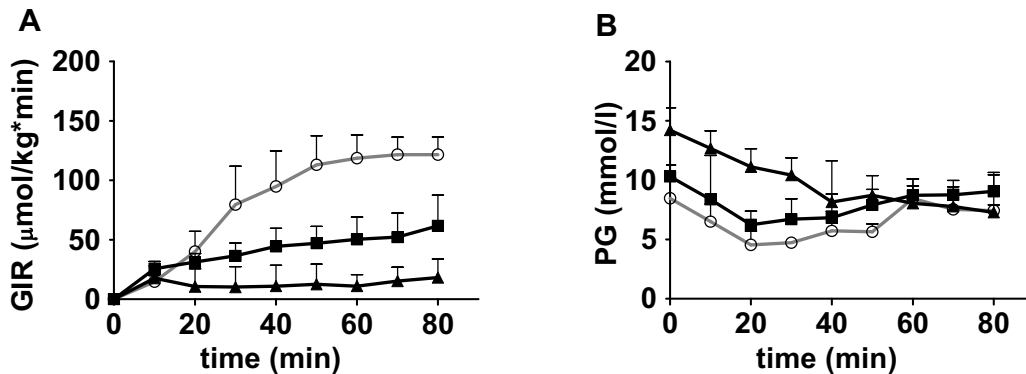


Figure 3: Clamp glucose infusion rates and plasma glucose levels; dynamic changes in (A) glucose infusion rates (GIR) and (B) plasma glucose levels (PG) during the clamp of ApoE3L mice fed a chow (open circles, grey line), HFBT (squares) or HFP (triangles) diet. Lines represent means \pm SD.

The effect of high fat diets on total liver lipid and cholesterol levels

Total liver lipid levels in the course of the diet interventions were determined. In HFP fed animals, liver TG content was significantly increased at 16 weeks, compared to chow fed animals. For HFBT fed animals, liver TG content was significantly increased at time points 12 and 16 weeks compared to chow fed animals. (HFP; 0.183 ± 0.125 , HFBT; 0.146 ± 0.047 , compared to chow; 0.096 ± 0.089 mmol/mg protein and HFP; 0.177 ± 0.087 , HFBT; 0.145 ± 0.055 , compared to chow; 0.051 ± 0.012 mmol/mg protein at 12 and 16 weeks, respectively, $p < 0.05$). No significant differences in liver TG content were found between the two high fat diet fed groups at any of the time points. Total liver cholesterol levels did not differ significantly between any of the groups at any of the time points measured (data not shown). These results indicate that after 16 weeks, both high fat diets induced hepatosteatosis compared to chow fed mice.

The effect of high fat diets on plasma proteins

A series of 71 plasma proteins were quantified at all time points of the time course, providing information on metabolism, inflammation, oxidation and related processes. Of these 71 plasma proteins, 48 proteins showed concentrations above the detection limit and were therefore included in the ASCA analysis. ASCA analysis showed a significant effect between the three diets ($p=0.041$), between the eight time points ($p=0.015$) as well as the interaction time*diet ($p=0.044$) explaining respectively 5.3%, 8.5% and 19.1% of the total variation in the data. Since ASCA did not reveal a significant difference between the two high fat diets, the "diet effect" on the plasma proteins is mainly due to the difference between the chow diet and the two high fat diets.

Table 3: Plasma proteins that contribute significantly to "diet" (D), "time" (T), or "diet*time" (I) effect in ApoE3L mice fed a chow, HFP or HFBT diet. Proteins which showed increased concentrations compared to chow fed controls are indicated with Up, proteins which showed decreased concentrations compared to chow fed controls are indicated with Down.

Protein	Symbol	Effect	Concentration
Apolipoprotein A1	Apo A1	D	Up
C Reactive protein	CRP	D, I	Up
Eotaxin		D, T	Up
Granulocyte Chemotactic Protein-2	GCP-2	T	Up
Haptoglobin		D, I	Up
Interleukin 10 (IL-10)	IL-10	D	Up
Interleukin-18	IL-18	I	Up
Interleukin-1 β	IL-1 β	D, T	Up
Interleukin-5	IL-5	T, I	Up
Leptin		D, T	Up
Lymphotactin		D	Down
Macrophage Inflammatory Protein-1 γ	MIP-1 γ	T, I	Down
Macrophage Inflammatory Protein-2	MIP-2	D	Up
Macrophage Inflammatory Protein-3 β	MIP-3 β	D	Up
Macrophage-Colony Stimulating Factor	M-CSF	D	Up
Monocyte Chemoattractant Protein-1	MCP-1	I	Up
Monocyte Chemoattractant Protein-3	MCP-3	D, I	Up
Myeloperoxidase (MPO)	MPO	D, I	Up
Serum Amyloid P	SAP	I	Up
Thrombopoietin (TPO)	TPO	D	Up
Tissue Factor		D	Up
Tissue Inhibitor of Metalloproteinase Type-1	TIMP-1	I	Up
Vascular Cell Adhesion Molecule-1	VCAM-1	D	Up

Table 3 shows the 23 proteins contributing to the diet, time and diet*time interaction effects. A number of proteins exhibited exclusively a diet effect which was predominantly characterized by increased plasma levels compared to chow. For example plasma apolipoprotein-A1 (Figure 4A), which was increased at day 1 on both high fat diets and remained increased at all time points of the time course. A number of proteins showed a diet*time interaction effect, mainly due to transiently increased plasma levels immediately after changing to the high fat diets on day 1-7, such as haptoglobin (Figure 4B). Interestingly, plasma leptin, showed both a diet and a time effect. The time effect was latter characterized by an increased level in both high fat diet groups beyond week 12 (Figure 4C).

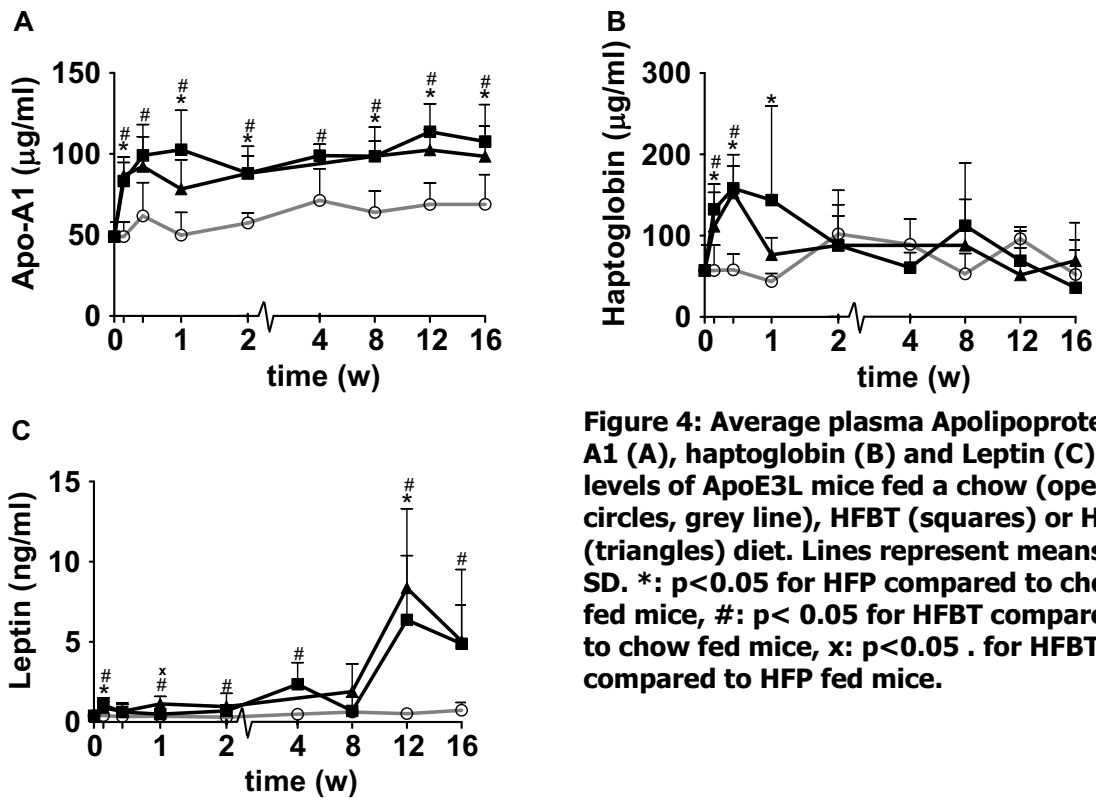


Figure 4: Average plasma Apolipoprotein-A1 (A), haptoglobin (B) and Leptin (C) levels of ApoE3L mice fed a chow (open circles, grey line), HFBT (squares) or HFP (triangles) diet. Lines represent means \pm SD. *: $p < 0.05$ for HFP compared to chow fed mice, #: $p < 0.05$ for HFBT compared to chow fed mice, x: $p < 0.05$. for HFBT compared to HFP fed mice.

Similar to haptoglobin, plasma levels of the proteins SAP, CRP, MCP-1, MCP-3, TIMP-1 and MIP-1gamma were transiently elevated after changing to the high fat diets. These results indicate that the switch to a high fat diet results in a transient increase in the plasma levels of a number of inflammatory/acute phase proteins.

The effect of high fat diets on the hepatic lipid profile

A series of 59 liver lipids and FFA species were quantified at all time points of the time course, providing information on lipid metabolism. ASCA analyses revealed a highly significant effect between the three diets ($p = 0$) and between the eight time points ($p = 0$) explaining respectively 22% and 15% of the total variation in

the data. The 'diet*time' interaction effect was not significant. As expected, exposure to high fat diets resulted in changed concentrations of several hepatic lipids. This time also a significant difference between the two high fat diets with regard to liver lipids was found, representing differences in the composition of the diets (data not shown).

Table 4: Liver lipids and fatty acids with a significant "time" effect in HFBT and HFP fed mice compared to chow fed controls.

Early phase	Effect	Intermediate phase	Effect	Late phase	Effect
		C20:3_FA	Up	C48:1_TG	Up
C16:1_FA	Down	C20:4_FA	Up	C48:2_TG	Up
C16:2_FA	Down	C24:5_FA	Down	C50:0_TG	Up
C20:0_FA	Down	C18:1_LPC	Up	C50:2_TG	Up
C20:1_FA	Down	C32:0_PC	Down	C52:2_TG	Up
C20:2_FA	Down	C36:3_PC	Up	C52:3_TG	Up
C16:0_LPC	Down	C46:0_TG	Down	C54:2_TG	Up
C18:0_LPC	Down	C52:4_TG	Down	C54:3_TG	Up
C18:3_LPC	Down	C52:5_TG	Down	C54:4_TG	Up
		C54:6_TG	Down	C56:5_TG	Up

Focusing on the hepatic lipids with a time-effect, ASCA was applied to the lipid profiling data set normalized for mice on control diet. The time effect explained 40% of the total variation in the data after normalization (p=0). The most prominent time-effect explained approximately 36% of the total time-effect, and was termed the "late phase". The second strongest time-effect explained approximately 29% of the total time-effect and was termed the "intermediate phase". The third time effect was termed the "early phase", and explained approximately 18% of the total time-effect (figure 5).

Table 4 summarizes the fatty acids and lipids that revealed a significant time-effect of both high fat diets in livers of ApoE3L mice. Concentrations of several free fatty acids and lysophosphatidylcholines were decreased in the early phase of the time-course (starting at week 1 and lasting up to 2 weeks). In the intermediate phase (weeks 4 and 8), increased and decreased concentrations of several lipid classes were found, while different triglyceride species showed a prominent accumulation in the late time phase (weeks 12 and 16). These results indicate that the liver lipid profile of high fat diet fed ApoE3L mice is characterized by three phases of homeostatic disturbances, which can be subdivided in an early, an intermediate and a late phase.

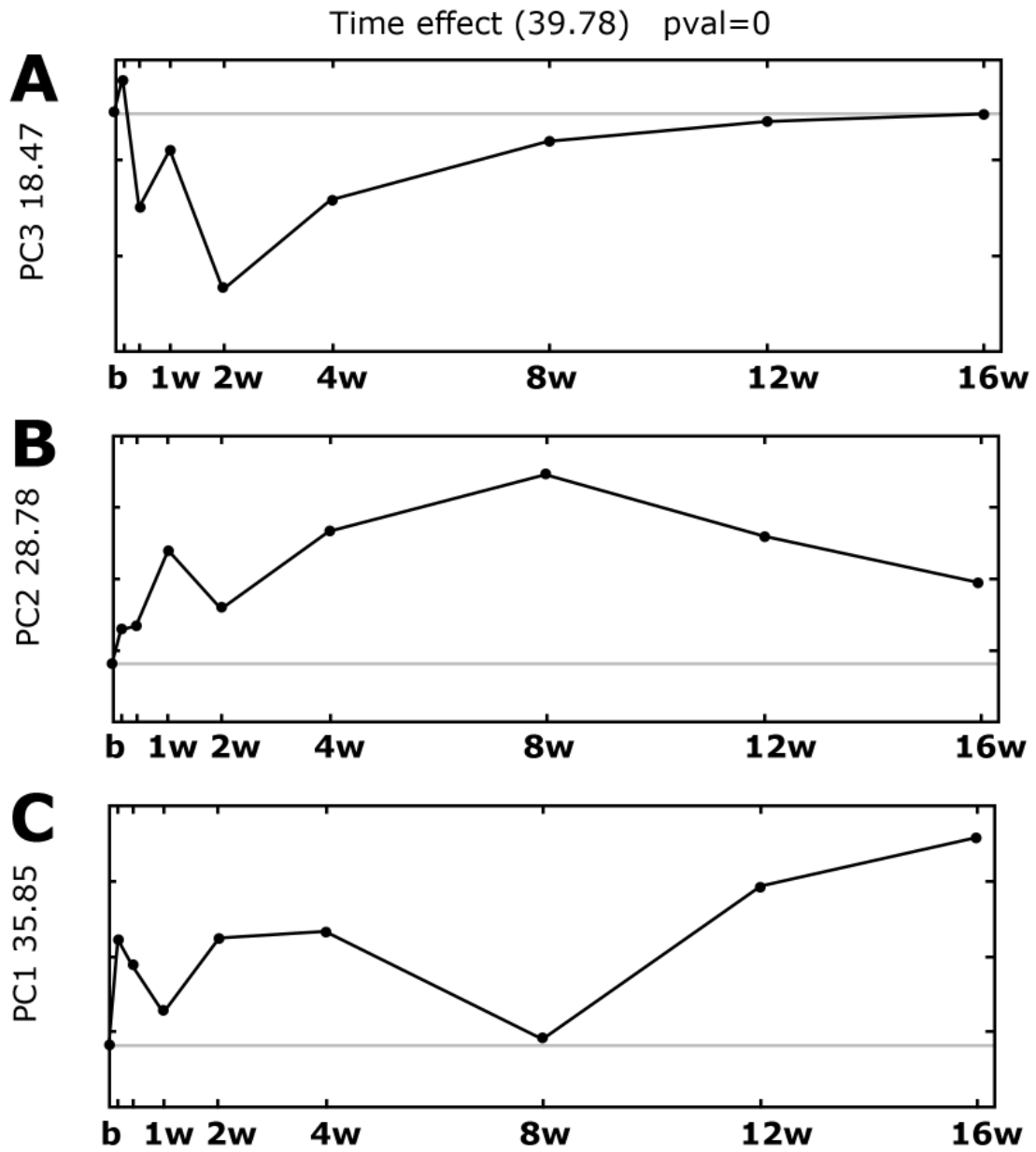


Figure 5: ASCA analysis on lipids profiling data of the ApoE3L mice on high fat diet, showing the early (A), intermediate (B) and late (C) oases. The values are relative to the median intensity of ApoE3L mice on chow diet per time point.

Differences in response between mice on HFBT and HFP diets

The overall hepatic lipid and plasma protein profile of ApoE3L mice responded similar to the HFBT and HFP diets. This is demonstrated by the lack of statistical significance in the time*diet interaction in the ASCA model for the hepatic lipid and the plasma protein profile normalized for mice on control diet (results not shown; $p = 0.5$ and 0.1 respectively).

Interestingly, the proportion of palmitoleoyl-LPC (C16:1-LPC) versus palmitoyl-LPC (C16:0-LPC) and oleoyl-LPC (C18:1-LPC) versus stearoyl-LPC (C18:0-LPC), as measures of the desaturation index, were found to be significantly increased in livers of ApoE3L mice on HFBT compared to chow, but not in HFP livers compared to chow (Figure 6A and 6B). Furthermore, both desaturation indices differed significantly between mice on HFBT and HFP from week 8 onwards. These data suggest that the activity of hepatic Stearoyl-CoA Desaturase 1 (SCD1) is higher in HFBT fed animals as compared to HFP and chow fed mice.

The hepatic n-6:n-3 PUFA ratio (the ratio between the concentrations of arachidonic acid and EPA) was found to be significantly elevated in livers of ApoE3L mice on both HF diets compared to chow. Interestingly, the hepatic n-6:n-3 PUFA ratio was significantly higher in ApoE3L mice on HFP compared to mice on HFBT (Figure 6C).

Hepatic diglycerides, sphingomyelin and ceramide contents

To further characterize the etiology of high fat diet induced hepatic lipid accumulation, concentrations of individual diglycerides (DG), sphingomyelins (SPM) and ceramides (CER) were measured at the 16 week time point. Total liver DG level was found to be significantly increased in ApoE3L mice on HFP ($p = 0.049$), whereas unchanged in ApoE3L mice on HFBT compared to chow controls (Chow 90.4 ± 26.0 HFBT; 152.9 ± 71 and HFP; 156 ± 60). Interestingly, total liver CER was found to be significantly decreased in ApoE3L mice on HFBT ($p = 0.004$), whereas unchanged in mice on HFP compared to chow controls (Chow 53 ± 19 , HFBT; 21 ± 7 and HFP; 32 ± 15 mmol/l). Total DG and CER contents, however, were not significantly different between ApoE3L mice on HFBT and HFP, suggesting that total DG and CER liver concentrations in ApoE3L mice on HFP follow the same trend as in mice on HFBT. Finally, total liver SPM was found to be significantly decreased in ApoE3L mice on both HF diets compared to chow controls (Chow 38 ± 5 , HFBT; 19 ± 5 and HFP; 27 ± 6 mmol/l, $p < 0.05$). In addition, SPM contents were significantly more reduced in HFBT fed animals compared to HFP fed animals. The ratio of total SPM to total CER was found to be identical in all conditions.

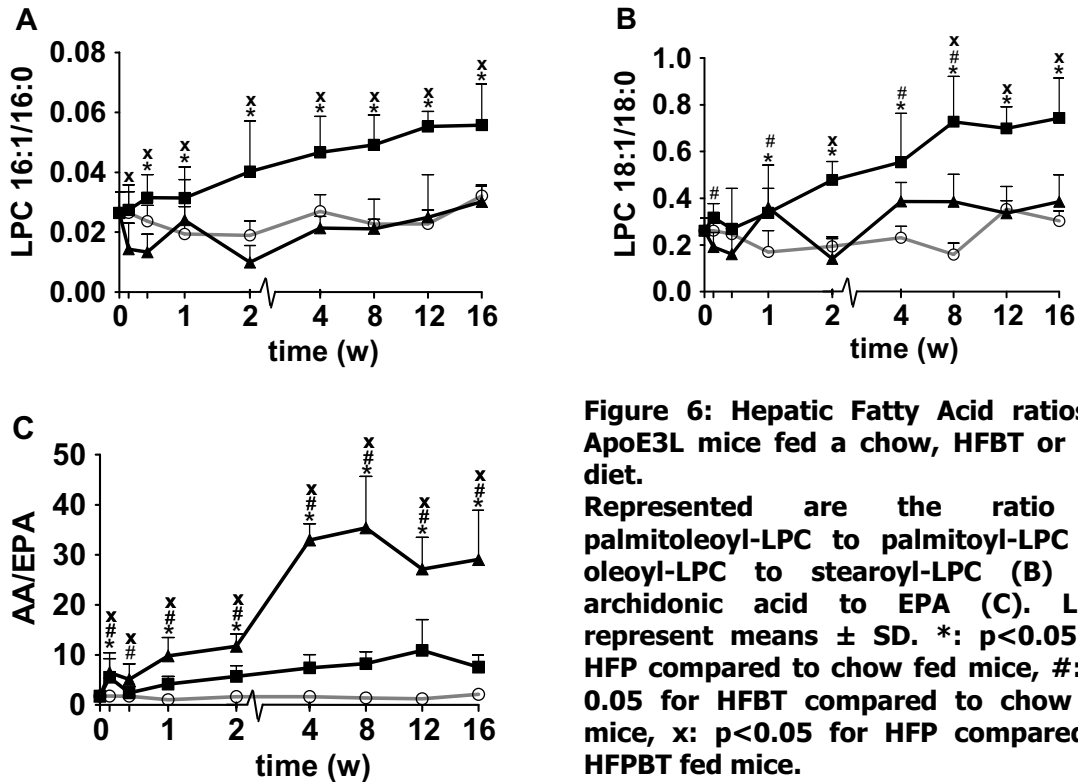


Figure 6: Hepatic Fatty Acid ratios in ApoE3L mice fed a chow, HFBT or HFP diet. Represented are the ratio of palmitoleoyl-LPC to palmitoyl-LPC (A) oleoyl-LPC to stearoyl-LPC (B) and arachidonic acid to EPA (C). Lines represent means \pm SD. *: $p < 0.05$ for HFP compared to chow fed mice, #: $p < 0.05$ for HFBT compared to chow fed mice, x: $p < 0.05$ for HFP compared to HFBT fed mice.

Discussion

In this study, we investigated the time dependent effects of two high fat diets on plasma lipid levels, plasma protein markers, liver lipid content, liver lipid composition, obesity and insulin sensitivity. All measurements were performed at high frequency over a 16 week intervention period to gain insight into the dynamics of the various responses. The results showed that the overall response to both high fat diets was characterized by three major phases: an early acute phase (day 1-week 2), an intermediate phase (weeks 4 and 8) and a late phase characterized by hepatic lipid accumulation (weeks 12 and 16). The phasing of these responses is in concordance with the phasing and responses that were found by liver transcriptomics analyses from the same experimental groups (198).

The early phase of the high fat diet response is characterized by a transient increase in acute phase protein markers such as haptoglobin, CRP and SAP and is therefore interpreted as an "acute" early phase inflammatory response. These acute phase proteins peak at day 1-7 and are back to normal levels beyond week 2. The ASCA analysis of the normalized liver lipids also showed significant perturbations in the first 2 weeks. In this early phase, a number of saturated (e.g. arachidic acid), omega-9 (e.g. palmitoleic acid) free fatty acids, as well as a number of the lysophosphatidylcholines showed decreased concentrations in the early phase (Table 4). Combined, these data clearly indicate that the switch to a

high fat diet invokes an acute phase inflammatory response and a number of transient changes in the hepatic lipidome.

In the intermediate phase, plasma levels of a number of protein markers are changed in the high fat diet fed groups as compared to the chow fed groups without major additional fluctuations. The ASCA analysis of the normalized liver lipids in time showed significant perturbations only for one principal component, which explains 29% of the time-variation. Several individual triglycerides, for example C52:4, C52:5 and C54:6, showed decreased concentrations in the intermediate phase (Table 4), which may be due to lower contents of these triglycerides in the HF diets compared to the control diet (Table 2). Furthermore, arachidonic acid (C20:4- ω 6), mead acid (C20:3- ω 9), and linoleic acid containing C36:3-PC showed increased concentrations in the intermediate phase, possibly due to the limited concentrations of ω 3 lipid sources in both HF diets. Omega -3, -6 and -9 fatty acid sources compete for the same desaturase and elongase enzymes, with a preference for the omega-3 fatty acid precursors. Therefore, when less omega-3 substrate is available, the production of desaturated and elongated ω 9 and ω 6 fatty acids and lipids containing these fatty acids will increase. Arachidonic acid (C20:4-FA), an omega 6 fatty acid, and the phosphatidylcholine C36:3-PC are known as pro-inflammatory eicosanoid precursors. C36:3-PC is an efficient substrate for mammalian lipoxygenases (114), which catalyze the biosynthesis of leukotrienes, lipoxins, and other lipid-derived mediators that are involved in a wide variety of pathophysiological processes, including inflammation. Therefore, one can speculate that during the intermediate phase, mice on both HF diets produce elevated concentrations of pro-inflammatory eicosanoid precursors, which later may result in pathology.

In the late phase, the mice on the high fat diet became more obese than the chow fed control mice. In parallel, plasma leptin was significantly increased in high fat fed mice (Fig 4C). This is indicative for resistance to anorexic effects of leptin. In the late phase, several TG species (Table 4) as well as total TG (Figure 4) showed increased concentrations in liver, indicating the development of mild hepatic steatosis. This is in line with a decreased action of leptin (11). In general, the TG available from the diet accumulated in the liver (Table 2 and 4). It should be noted that hepatic transcriptome analysis indicated the activation of a steatotic transcriptional program mediated by the adipocyte transcription factor PPAR γ in the late phase (198). These data all point towards a phenotype aimed at lipid accumulation.

Interestingly, statistical analyses showed similar responses in both high fat diets in the overall hepatic lipid and plasma protein response, as well as many physiological parameters and hepatic transcripts (198). Some differences between the responses of the two high fat diets were found, especially in the hepatic content of specific lipids. As compared to the HFBT diet, the HFP diet

induced increased hepatic levels of n-6 over n-3 PUFA. This might be due to relatively higher contents of linoleic acid (C18:2n6) in the HFP diet. Since the n-6:n-3 PUFA ratio can be interpreted as the ratio between pro- and anti-inflammatory eicosanoid precursors, these data suggest that both HF diets, but HFP in particular, increase inflammation.

Secondly, the HFP diet significantly increased the hepatic levels of saturated versus mono-unsaturated LPC. It has been shown that increases of these LPC desaturation indices are due to increased activity of hepatic SCD-1 (42). Unfortunately, LPCs were the only hepatic lipid class measured containing monounsaturated fatty acids, so it was not possible to determine whether this finding is general for all hepatic lipid classes. It is unlikely that differences in these desaturation indexes reflect differences in dietary fatty acid intake. Indeed, the dietary HFBT C16:1/C16:0 FA ratio is 16 times higher compared to HFP, but the dietary C18:1/C18:0 ratio is 3 times higher in HFP compared to HFBT. If differences in hepatic LPC desaturation indices would be a mirror of dietary fatty acid intake, than significant differences in LPC desaturation indexes between animals on HFP and chow were also to be expected. Therefore, these findings were interpreted to be due to increased activity of hepatic SCD-1 in ApoE3L mice on HFBT versus the mice on HFP and chow diet. The increased activity of SCD-1 may be caused by higher contents of stearic acid (C18:0) in the HFBT diet compared to HFP and chow, which is the preferred substrate for SCD-1 (213). Because hepatic SCD-1 activity is associated with the development of hepatic insulin resistance (77), this would indicate a lower insulin sensitivity in the liver of HFBT fed animals compared to HFP. This is in line with previous data, where a diet rich in animal fat induced a higher degree of hepatic insulin resistance compared to a diet rich in plant fat (250). In addition, increased activity of SCD-1 can explain decreased hepatic synthesis of CER and SPM in ApoE3L mice on HFBT as synthesis of CER is highly dependent on availability of palmitic acid (231).

In conclusion, our analyses of the response of APOE3L mice to two different HF diets demonstrate that the overall response of plasma protein markers and hepatic lipids was very similar in time. Both HF diets showed a three-phased response in combined plasma protein and hepatic lipid profiles that was also found in the transcriptomics analyses. These data indicate that the development of diet induced pathology is not a linear response but rather is characterized by dynamic cycles of responses. This implies that the timing of an experiment needs to be carefully considered and chosen, since this will affect the processes that will be occurring. Only a few specific hepatic lipids showed differences between ApoE3L mice on the two high fat diets. Whether these differences in lipid and fatty acid profiles are causally related to the severity of impaired insulin sensitivity remains to be determined.